Enhanced Stability of a Paramagnetic Palladium Complex Promoted by Interactions with Ethynyl Substrates

Sophie Dal Molin,[†] Cyril Cugnet,[†] David Brevet,[†] Dominique Lucas,[†] Yves Mugnier,*[,†] Daniel Fortin,[‡] René T. Boeré,*[,§] and Pierre D. Harvey*[,‡]

Institut de Chimie Moléculaire de l'Université de Bourgogne (ICMUB), UMR CNRS 5260, Faculté des Sciences Mirande, Université de Bourgogne, 9 Avenue Alain Savary, BP 47870, 21078 Dijon Cedex, France, Département de Chimie, Université de Sherbrooke, Sherbrooke J1K 2R1, Québec, Canada, and the Department of Chemistry and Biochemistry, University of Lethbridge, Lethbridge T1K 3M4, Alberta, Canada

Received April 18, 2007

The highly reactive palladium-centered radical cluster $[Pd_3(dppm)_3(CO)]^{\bullet+}$ exhibits only a limited stability in solution at room temperature (about an hour). This stability can be extended significantly to several hours by adding organic substrates such as the symmetric and asymmetric alkynes Ph−C≡C−H and $MeO_2C-C\equiv C-CO_2Me$, which reversibly bind to the Pd_3 triangle. The presence of the substrate inside the cavity protects the palladium centers from reacting with the "outside world", hence enhancing the stability. Both adducts are stable as the cluster is always totally recovered. The paramagnetic complexes along with their corresponding dications were characterized by EPR, variable-temperature ^{31}P NMR, UV−vis and MALDI-TOF spectroscopy, and electrochemistry. For the $MeO_2C-C\equiv C-CO_2Me/[Pd_3(dppm)_3(CO)]^{2+}$ complex, the analysis of the low-temperature ^{31}P NMR spectra strongly suggests a major structure modification of the ligand and substrate with respect to the starting materials.

Introduction

Palladium-containing organometallic and coordination complexes continue to be extremely important species in homogeneous catalysis.[1] Attempts to model the catalytic reactivity at surfaces using polymetallic clusters and related derivatives were made.[2,3] Recently, our research teams investigated the first confidently characterized paramagnetic palladium species, the cyclic unsaturated $[Pd_3(dppm)_3(CO)]^{\bullet+}$ cluster,[4] along with its electrochemical reactivity toward the stoichiometric and catalytic activation of various organic compounds, such as halocarbons and acid halides,[5−8] and inorganics, such as I^-, PF_6^-, BF_4^-, OH^-, and H^-.[9,10] While one paramagnetic binuclear palladium complex is known ($[Pd_2(\mu\text{-PhCCPh})(\eta\text{-}C_5Ph_5)_2]^{\bullet+}$),[11−13] the title cluster remains a rare example of a metal-centered paramagnetic cluster. The only other example of a paramagnetic palladium-cluster, to our knowledge, is the giant aggregate $Pd_{561}(phen)_{36}(O)_{200}$ (phen = phenanthroline).[14] In relation with this work, one of us also recently investigated the paramagnetic binuclear complex $[Pt_2(\mu\text{-}\kappa As,\kappa C\text{-}C_6H_3\text{-}5\text{-Me-}2\text{-}AsPh_2)_4]^{\bullet+}$.[15] Hetero-polymetallic systems that exhibit paramagnetic properties also exist, and again the number of examples is also relatively small and include binary and ternary inorganic polymers such as $PdAs_2O_6$,[16] LnPdSi (Ln = La, Ce, Pr),[17] Eu_2PdH_x ($x = 0.1-4$),[18] $M_4Pd_{10}In_{21}$ (M = La, Ce, Pr, Nd, Sm),[19] $CaMIn_2$ (M = Pd, Pt, Au),[20] $Pd_7Sn_2Se_{9.85}$,[21] $Pd_{13}Te_{13}$[22]), metal−metal-bonded 1-D hetero bi- and polynuclear complexes ($[Pt_2Pd(A_2)_2(L)_4]^{3+}$ (L = 1-methyl-

* To whom correspondence should be addressed. (Y.M.) Tel and Fax: (+33) 03-80-39-60-91. E-mail: Yves.Mugnier@u-bourgogne.fr. (R.T.B.) E-mail: boere@uleth.ca. (P.D.H.) Tel: (+1) 819-821-7092. Fax: (+1) 819-821-8017. E-mail: Pierre.Harvey@USherbrooke.ca.

[†] ICMUB.

[‡] Université de Sherbrooke.

[§] University of Lethbridge.

(1) Tsuji, J., Ed. Palladium in Organic Synthesis. In *Topics in Organometallic Chemsitry*; Springer GmbH: Berlin, Germany, 2005; Vol. 14, p 332.

(2) Puddephatt, R. J.; Xiao, J. *NATO ASI Ser. Ser. C* **1996**, *474*, 407−435.

(3) Puddephatt, R. J. *Met. Clusters Chem.* **1999**, *2*, 605−615.

(4) Brevet, D.; Lucas, D.; Cattey, H.; Lemaitre, F.; Mugnier, Y.; Harvey, P. D. *J. Am. Chem. Soc.* **2001**, *123*, 4340−4341.

(5) Lemaitre, F.; Lucas, D.; Mugnier, Y.; Harvey, P. D. *J. Org. Chem.* **2002**, *67*, 7537−7540.

(6) Brevet, D.; Mugnier, Y.; Lemaitre, F.; Lucas, C. D.; Samreth, S.; Harvey, P. D. *Inorg. Chem.* **2003**, *42*, 4909−4917.

(7) Lemaitre, F.; Lucas, D.; Groison, K.; Richard, P.; Mugnier, Y.; Harvey, P. D. *J. Am. Chem. Soc.* **2003**, *125*, 5511−5522.

(8) Lucas, D.; Lemaitre, F.; Gallego-Gomez, B.; Cugnet, C.; Richard, P.; Mugnier, Y.; Harvey, P. D. *Eur. J. Inorg. Chem.* **2005** (6), 1011−1018.

(9) Lemaitre, F.; Brevet, D.; Lucas, D.; Vallat, A.; Mugnier, Y.; Harvey, P. D. *Inorg. Chem.* **2002**, *41*, 2368−2373.

(10) Cugnet, C.; Lucas, D.; Lemaitre, F.; Collange, E.; Soldera, A.; Mugnier, Y.; Harvey, P. D. *Chem.−Eur. J.* **2006**, *12*, 8386−8395.

(11) Connelly, N. G.; Geiger, W. E.; Orpen, A. G.; Orsini, J. J., Jr.; Richardson, K. E. *J. Chem. Soc., Dalton Trans.* **1991** (11), 2967−2977.

(12) Broadley, K.; Lane, G. A.; Connelly, N. G.; Geiger, W. E. *J. Am. Chem. Soc.* **1983**, *105*, 2486−2487.

(13) Broadley, K.; Connelly, N. G.; Lane, G. A.; Geiger, W. E. *J. Chem. Soc., Dalton Trans.* **1986** (2), 373−376.

(14) Van Ruitenbeek, J. M.; Jurgens, M. J. G. M.; Schmid, G.; Van Leeuwen, D. A.; Zandbergen, H. W.; De Jongh, L. J. *Z. Phys. D: At. Mol. Clusters* **1991**, *19*, 267−270.

(15) Bennett, M. A.; Bhargava, S. K.; Boas, J. F.; Boeré, R. T.; Bond, A. M.; Edwards, A. J.; Guo, S.-X.; Hammerl, A.; Pilbrow, J. R.; Priver, S. H.; Schwerdtfeger, P. *Inorg. Chem.* **2005**, *44*, 2472−2482.

(16) Orosel, D.; Jansen, M., *Z. Anorg. Allg. Chem.* **2006**, *632*, 1131−1133.

(17) Prots, Y. M.; Jeitschko, W.; Gerdes, M.; Kuennen, B. *Z. Anorg. Allg. Chem.* **1998**, *624*, 1855−1862.

(18) Kohlmann, H.; Fischer, H. E.; Yvon, K. *Inorg. Chem.* **2001**, *40*, 2608−2613.

(19) Zaremba, V. I.; Rodewald, U. C.; Kalychak, Y. M.; Galadzhun, Y. V.; Kaczorowski, D.; Hoffmann, R.-D.; Poettgen, R. *Z. Anorg. Allg. Chem.* **2003**, *629*, 434−442.

(20) Hoffmann, R.-D.; Pottgen, R.; Landrum, G. A.; Dronskowski, R.; Kunnen, B.; Kotzyba, G. *Z. Anorg. Allg. Chem.* **1999**, *625*, 789−798.

(21) Pocha, R.; Johrendt, D. *Z. Anorg. Allg. Chem.* **2004**, *630*, 2468−2472.

(22) Janetzky, M.; Harbrecht, B. *Z. Anorg. Allg. Chem.* **2006**, *632*, 837−844.

10.1021/om700377a CCC: $37.00
Publication on Web 09/11/2007

Chart 1. Schematic Representation of Cluster/Alkyne Interaction (n = 0, 1, 2)

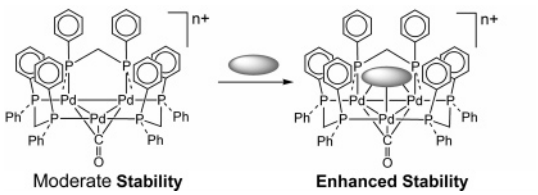

uracylato, 1-methylthyminato; A_2 = 2 NH_3, en)[23]), one cluster ($[Ni_{16}Pd_{16}]^{4-}$),[24] and nonmetal−metal-bonded bi- and trinuclear species ($[I_2Rh(p\text{-}tolN_3tol\text{-}p)_2Pd(\eta^3\text{-}C_3H_5)]^-$[25] and $[(Ln)Ru(\mu\text{-}S(CH_2CH_2S)_2)_2]^{2+}$ (Ln = Me_6C_6; Me_5C_5).[26] In the latter cases, the odd electrons are located on the rhodium and ruthenium metals, not the palladium. These literature reports on stable paramagnetic palladium-containing materials suggest that their stability is related to cooperative effects, either by electron delocalization or by electron localization on a different type of metal atom where the presence of the odd electron does not induce instability.

The title paramagnetic cluster is a persistent radical that is sufficiently stable for *ex situ* characterization by EPR spectroscopy, but is mostly decomposed after 1 h at room temperature. Its relative stability is also attributable to the delocalization of the single electron over the three metal and six phosphorus atoms and the protective cavity formed by an array of dppm-phenyl groups surrounding the unsaturated Pd_3 center (the other side of which is protected by the μ_3-CO ligand).[27,28] We now report adducts of a symmetrical, electron-deficient, dimethylacetylene dicarboxylate ($MeO_2C-C\equiv C-CO_2Me$) and an unsymmetrical phenylacetylene ($Ph-C\equiv C-H$) substrate with the $[Pd_3(dppm)_3(CO)]^{n+}$ clusters (Chart 1), in which n may equal 2 (diamagnetic, characterizable by NMR) or 1 (paramagnetic, characterizable by EPR). The paramagnetic clusters are stable for several hours at room temperature in the absence of oxygen, suggesting that the presence of alkyne in the cavity formed by the dppm phenyl groups reduced the reactivity of the unpaired electron. The evidence we have obtained so far indicates considerable variation in the nature of the alkyne−metal interactions depending on the presence or absence of electron-withdrawing and/or bulky substituents on the C≡C unit. We suggest that the importance of nonbonding interactions between the array of dppm phenyl groups and the incoming alkynes should not be overlooked (Chart 1); hence in addition to specific bonding to the Pd_3 surface, nonclassical interactions normally associated with "host−guest" chemistry may play a role.

Results and Discussion

Reversible Adduct Formation. The formation of $[Pd_3(dppm)_3(CO)]^{2+}$ adducts (Chart 1 when n = 2), as PF_6^- salts, with $MeO_2C-C\equiv C-CO_2Me$ or $Ph-C\equiv C-H$ in THF (the choice of solvent is important) is demonstrated by UV−vis spectroscopy (Figure 1). Evidence for reversible coordination

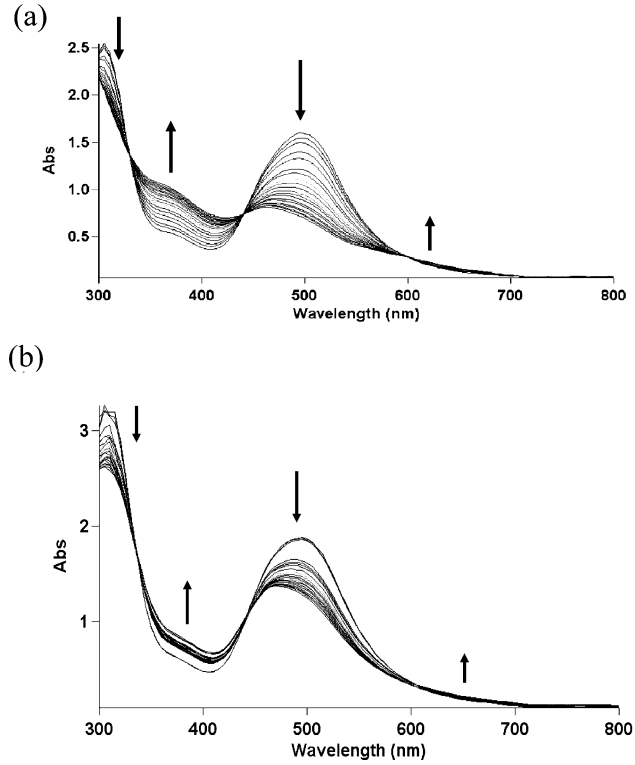

Figure 1. Evolution UV−vis spectra of $[Pd_3(dppm)_3(CO)]^{2+}$ (as a PF_6^- salt) upon the addition of $Ph-C\equiv C-H$ (a) and $MeO_2C-C\equiv C-CO_2Me$ (b) up to 2 equiv in THF at room temperature. Each addition represents 0.1 equiv.

Chart 2

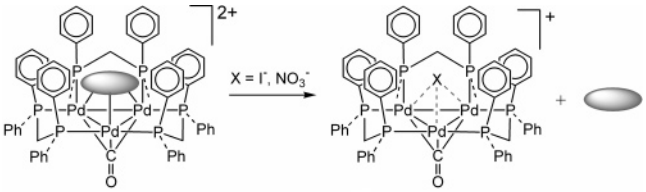

is demonstrated by the addition of 1 equiv of I^- or NO_3^- ions into adduct-containing solutions (Chart 2), which leads to competitive reactions where the anion quantitatively displaces the neutral substrates to form the known adducts $[Pd_3(dppm)_3(CO)(X)]^+$ with X = I^- or NO_3^-; these reactions can be reliably followed by ^{31}P NMR, UV−vis, and cyclic voltammograms (CV) as verified against authentic samples.[9,29]

Constants of formation, K_F, as measured from the Scott's and Scatchard's plots[30] are 85 000 (±5000) and 4500 (±1000) M^{-1} for $Ph-C\equiv C-H$ and $MeO_2C-C\equiv C-CO_2Me$, respectively. Such constants indicate very strong binding for these neutral species in comparison with various aromatic rings and solvent molecules (benzene, toluene, acetonitrile, nitrobenzene, and benzonitrile for example; $0.07 < K_F < 2\ M^{-1}$).[31] In fact, these values compare favorably to that found for carboxylate derivatives (730−10 000 M^{-1}),[31] which are considered weak anionic binders. These values are also consistent with the fact that the ethynyl guests are competitively removed by the strong binders such as I^- and NO_3^-. $\pi-\pi$ interactions cannot alone explain

(23) Micklitz, W.; Mueller, G.; Huber, B.; Riede, J.; Rashwan, F.; Heinze, J.; Lippert, B. *J. Am. Chem. Soc.* **1988**, *110*, 7084−92.
(24) Ricco, M.; Shiroka, T.; Carretta, S.; Bolzoni, F.; Femoni, C.; Iapalucci, M. C.; Longoni, G. *Chem.−Eur. J.* **2005**, *11*, 2856−2861.
(25) Adams, C. J.; Baber, R. A.; Connelly, N. G.; Harding, P.; Hayward, O. D.; Kandiah, M.; Orpen, A. G. *Dalton Trans.* **2006** (14), 1749−1757.
(26) Shin, R. Y. C.; Tan, G. K.; Koh, L. L.; Goh, L. Y.; Webster, R. D. *Organometallics* **2004**, *23*, 6108−6115.
(27) Harvey, P. D.; Mugnier, Y.; Lucas, D.; Evrard, D.; Lemaitre, F.; Vallat, A. *J. Cluster Sci.* **2004**, *15*, 63−90.
(28) Puddephatt, R. J.; Manojlovic-Muir, L.; Muir, K. W. *Polyhedron* **1990**, *9*, 2767−2802.
(29) Brevet, D.; Lucas, D.; Richard, P.; Vallat, A.; Mugnier, Y.; Harvey, P. D. *Can. J. Chem.* **2006**, *84*, 243−250.
(30) Connors, K. A. *Binding Constants: The Measurements of Molecular Complex Stability*; John Wiley & Sons: New York, NY, 1987.
(31) Provencher, R.; Aye, K. T.; Drouin, M.; Gagnon, J.; Boudreault, N.; Harvey, P. D. *Inorg. Chem.* **1994**, *33*, 3689−3699.

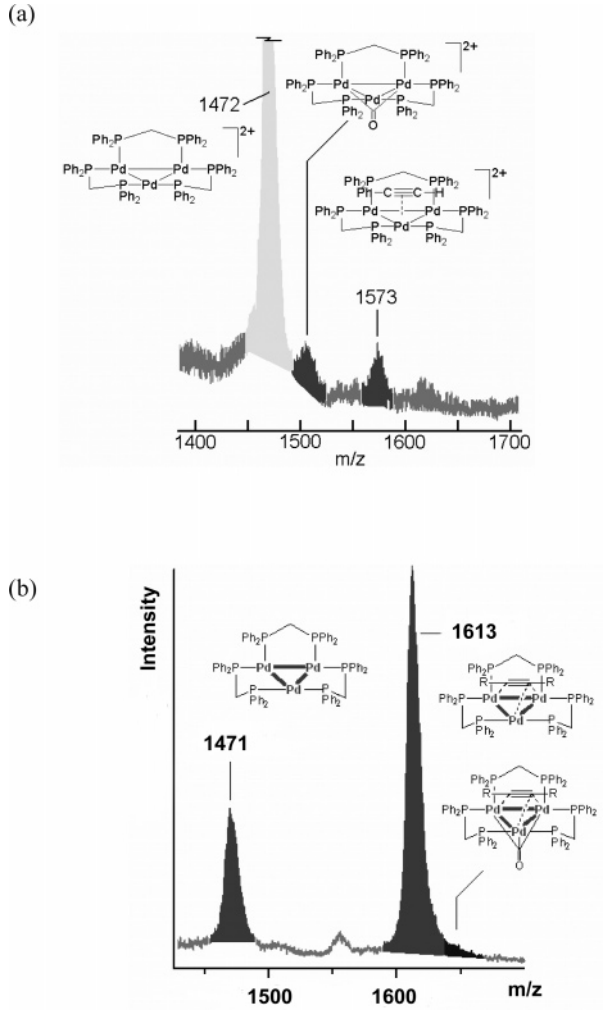

Figure 2. MALDI-TOF signals (a) in the 1400 to 1700 region of the Ph−C≡C−H/$[Pd_3(dppm)_3(CO)]^{2+}$ and (b) in the 1400 to 1800 region of the $MeCO_2$−C≡C−CO_2Me/$[Pd_3(dppm)_3(CO)]^{2+}$ adducts.

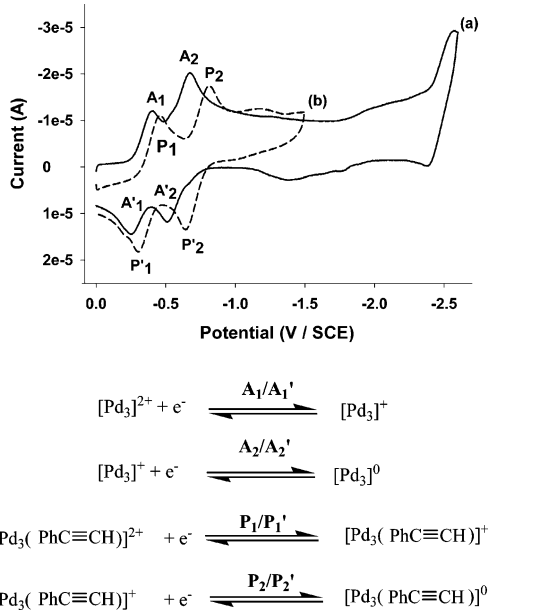

(c)

$[Pd_3]^{2+} + e^- \rightleftharpoons [Pd_3]^+$ (A_1/A_1')

$[Pd_3]^+ + e^- \rightleftharpoons [Pd_3]^0$ (A_2/A_2')

$[Pd_3(PhC{\equiv}CH)]^{2+} + e^- \rightleftharpoons [Pd_3(PhC{\equiv}CH)]^+$ (P_1/P_1')

$[Pd_3(PhC{\equiv}CH)]^+ + e^- \rightleftharpoons [Pd_3(PhC{\equiv}CH)]^0$ (P_2/P_2')

Figure 3. (a) Cyclic voltammogram of $Pd_3(dppm)_3(CO)^{2+}$ (—) in THF in the presence of 0.2 mol·L^{-1} of Bu_4NPF_6; (b) after addition of 5 equiv of Ph−C≡C−H (----). Starting potential is 0 V vs SCE; sweep rate is 100 mV·s^{-1}. (c) $[Pd_3]^{n+}$ and $[Pd_3(Ph{-}C{\equiv}C{-}H)]^{n+}$ denote $Pd_3(dppm)_3(CO)^{n+}$ and $Pd_3(dppm)_3(CO)(Ph{-}C{\equiv}C{-}H)^{n+}$, respectively.

Chart 3[a]

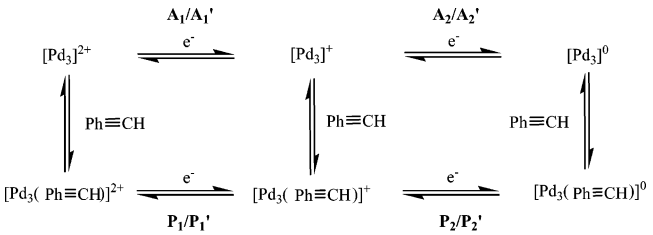

[a] $[Pd_3]^{2+} = [Pd_3(dppm)_3(CO)]^{2+}$.

such large values for neutral species. Evidence for ethynyl−palladium interactions is provided below.

Further evidence for adduct formation is provided by MALDI-TOF; the adducts $MeO_2C{-}C{\equiv}C{-}CO_2Me$//$[Pd_3(dppm)_3(CO)]^{2+}$ and Ph−C≡C−H/$[Pd_3(dppm)_3(CO)]^{2+}$ (as PF_6^- salts; Figure 2) exhibit unambiguous signals associated with the addition of the neutral organic substrate to the cluster in comparison with the starting material.

Corroboration for alkyne adduct formation is further provided by electrochemistry. The parent cluster, $[Pd_3(dppm)_3(CO)]^{2+}$ (as its PF_6^- salt), exhibits two reversible one-electron reduction waves at −0.21 and −0.47 V vs SCE (THF/0.2 mol·L^{-1} Bu_4NPF_6), corresponding to sequential one-electron reductions of the dication to the monocation and on to the neutral cluster (Figure 3).[32] In the Ph−C≡CH adduct, the reduction waves in CV remain reversible, but are shifted toward more negative potentials of −0.27 and −0.61 V vs SCE, respectively. On the other hand, in the $MeO_2C{-}C{\equiv}C{-}CO_2Me$ adduct, the equally reversible waves are shifted toward more positive potentials of −0.10 and −0.40 V vs SCE. On the assumption that back-bonding from the Pd to the alkyne becomes more important as the oxidation state is lowered, we can explain the changes in the observed potentials, in terms of the strong π-acceptor ability of dimethylacetylene dicarboxylate. Phenyl acetylene, on the other hand, exhibits a poorer π-acceptor capability, rendering reduction of its adduct more difficult than that of the parent cluster.

We also monitored the RDE traces for the electrogenerated $[Pd_3(dppm)_3(CO)]^{n+}$ ($n = 0, 1$) upon addition of Ph−C≡C−H to the solution. A typical experiment can be exemplified as follow: the $[Pd_3(dppm)_3(CO)]^{\bullet+}$ exhibits oxidation and reduction waves A_1' and A_2, respectively, become oxidation and reduction signals P_1' and P_2, respectively, upon addition of Ph−C≡C−H. The overall electrochemical investigations allow one to describe the addition/elimination behavior as a square scheme as presented in Chart 3. All in all, this work shows that in the presence of PF_6^- counteranion, the favored path in Chart 3 is $[Pd_3]^{2+} \rightarrow [Pd_3(Ph{-}C{\equiv}C{-}H)]^{2+} \rightarrow [Pd_3(Ph{-}C{\equiv}C{-}H)]^{+} \rightarrow [Pd_3(Ph{-}C{\equiv}C{-}H)]$.

Structural Characterization of the Dications. Despite considerable effort, we have so far been unable to obtain suitable crystals for a crystallographic study. Thus, we have characterized the structures of the diamagnetic adducts of the dications by ^{31}P NMR. In contrast to the spectra of the decarbonylated monocation $[Pd_3(dppm)_3(O_2CCF_3)(MeO_2C{-}C{\equiv}C{-}CO_2Me)]^+$

(32) Gauthron, I.; Mugnier, Y.; Hierso, K.; Harvey, P. D. *Can. J. Chem.* **1997**, *75*, 1182−1187.

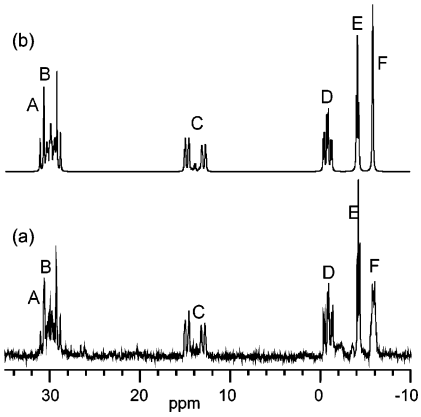

Figure 4. 243 MHz ^{31}P NMR spectrum at 220 K in the region of the complex $[Pd_3(dppm)_3(CO)(MeO_2C-C\equiv C-CO_2Me)]^{2+}$ cation. Experimental (a) and simulation using MestReC 4.9.9.9 (b). Simulation parameters: Lorentzian lines, line width = 15 Hz; ABCDEF spin system, $\delta_A = 30.0$, $\delta_B = 30.0$, $\delta_C = 13.9$, $\delta_D = -0.8$, $\delta_E = -4.2$, $\delta_F = -5.8$; $J_{AC} = 102$, $J_{AD} = 430$, $J_{BD} = 112$, $J_{BE} = 38$, $J_{BF} \approx 12$, $J_{CD} = 99$, $J_{CF} \approx 15$, $J_{DE} = 38$, $J_{EF} \approx 5$ Hz. Note that the line shape of the F signal (highest field) is not fully reproduced.

reported by Rashidi et al.[33] to be invariant over the temperature range −80 to +60 °C, both of our adducts—which retain CO as a cluster ligand—are evidently fluxional at ambient temperature. However, on cooling to 220 K, a fully resolved spectrum of $[Pd_3(dppm)_3(CO)(MeO_2C-C\equiv C-CO_2Me)]^{2+}$ and a partially resolved spectrum of $[Pd_3(dppm)_3(CO)(Ph-C\equiv C-H)]^{2+}$ could be obtained. As a starting point for discussion we review the spectral results of $[Pd_3(dppm)_3(O_2CCF_3)(MeO_2C-C\equiv C-CO_2Me)]^{+}$ because these workers also obtained an X-ray crystal structure of a solvated PF_6^- salt of this monocation (note that here the μ_3-CO ligand has been displaced by an η^1-trifluoroacetate ligand, rendering their monocation isolectronic with our dications.) Rashidi et al. report six distinct dppm ^{31}P signals of equal intensity with $\delta = 26.5$ ($J_{PP} = 96$, 43, 24 Hz), 20.7 ($J_{PP} = 435$, 97, 21 Hz), 16.9 ($J_{PP} = 435$, 95, 22 Hz), and −1.4, −2.6, −4.1 (unresolved multiplets). The large 435 Hz value indicative of *trans* coupling agrees well with the X-ray structure in which one of the three Pd atoms is coordinated by the trifluoroacetate and to one of the alkyne C atoms through σ-bonding, with the phosphorus atoms of two different dppm ligands in a close-to-square-planar disposition; the remaining Pd atoms display *cisoid* arrangements of the coordinated phosphorus atoms.[33]

The spectrum of $[Pd_3(dppm)_3(CO)(MeO_2C-C\equiv C-CO_2Me)]^{2+}$ at 220 K is quite similar, though not identical, to this spectrum (Figure 4). There are also six P signals of equal intensity, but two have (coincidentally) equivalent chemical shifts, generating an ABCDEF spin system: $\delta_A = 30.0$ ($J_{PP} = 430$, 102 Hz); $\delta_B = 30.0$ ($J_{PP} = 112$, 102, 38, ∼12 Hz); $\delta_C = 13.9$ ($J_{PP} = 430$, 99, ∼15 Hz); $\delta_D = -0.8$ ($J_{PP} = 112$, 99, 38 Hz); $\delta_E = -4.2$ ($J_{PP} = 38$, ∼5); $\delta_F = -5.8$ (unresolved multiplet). There is a 430 Hz *trans* coupling between the A and C signals, indicative of a single Pd center with square-planar geometry that is strikingly similar to that observed in $[Pd_3(dppm)_3(CO)(MeO_2C-C\equiv C-CO_2Me)]^{+}$, despite the difference in ligand set. One way that our dication could adopt such a structure with a single square-planar Pd center would be for the μ_3-CO to migrate to a terminal position. The structure

Chart 4

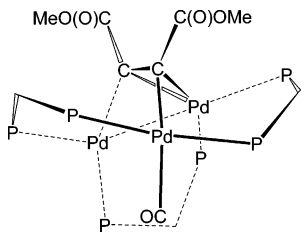

proposed is shown in the following line diagram, which was generated directly from the published crystal structure by Rashidi et al. through replacement of the coordinated trifluoroacetate by an η^1-CO group. (Note that in this view, displacement of the alkyne by an incoming anion would have the versatile carbonyl ligand returning to its μ_3-position.) There are no crystal structures of Pd complexes in which CO is *trans* to an X ligand and *cis* to two phosphines according to the Cambridge Structure Database (version 5.28, November 2006). However, related Pt(II) complexes are known in which CO is *trans* to CH_3 in a binuclear dppm "A-frame" complex,[34] *trans* to Cl in a monomeric complex,[35] *trans* to σ-acyl complexes,[36,37]a σ-cyclopentadienyl,[38] and a σ-vinyl complex.[39] All in all, these findings witnessing strong interactions could also be associated with substrate activation, which turns out to be reversible in this work.

Upon warming, the ^{31}P NMR spectra of this complex display evidence of some alteration in chemical shifts (the largest changes occurring for the A′ and E signals), and a general loss of signal intensity near room temperature is indicative of fluxionality, but whether this is between an alkyne-coordinated and uncoordinated monocationic complex or the complex becomes fluxional but retains coordinated alkyne is not apparent.

The ^{31}P NMR spectrum of $[Pd_3(dppm)_3(CO)(Ph-C\equiv C-H)]^{2+}$ is also fluxional (Figure 5) and remains significantly unresolved even at 200 K. There are three groups of signals of equal intensity at +21, −4.5, and −7 ppm, suggesting C_s symmetry for this cluster, unlike the dimethyl acetylene dicarboxylate complexes discussed above. Our interpretation is based on an AA′BB′CC′ spin system, and while the assignment of the peaks in Figure 5 is only tentative, it is consistent. We propose that the cluster undergoes a complex dynamic exchange, whereby the sharp signal assigned to BB′ is already in fast exchange at 220 K. This signal has been simulated using MestReC with spin−spin coupling of 95 Hz to one, 56 Hz to one, and 40 Hz to two equivalent phosphorus nuclei, and a line width of 10 Hz (Figure 5b). At this temperature the AA′ and CC′ signals are entering fast exchange, likely with each other. At 250 K, the simulation of the BB′ multiplet still fits the same parameters, but the line width increases to 30 Hz, and by RT the BB′ and CC′ signals have collapsed together. The AA′ and CC′ signals never sharpen fully before the exchange with BB′ commences. This is indicative of wholesale exchange in which the two signals that are close in frequency are coalesced but the AA′ signals remain distinct because of the larger frequency

(33) Rashidi, M.; Schoettel, G.; Vittal, J. J.; Puddephatt, R. J. *Organometallics* **1992**, *11*, 2224−2228.

(34) Hutton, A. T.; Shabanzadeh, B.; Shaw, B. L. *J. Chem. Soc., Chem. Commun.* **1983** (19), 1053−1055.

(35) Rusakov, S. L.; Lysyak, T. V.; Apal'kova, G. M.; Gusev, A. I.; Kharitonov, Y. Y.; Kolomnikov, I. S. *Koord. Khim.* **1988**, *14*, 229−233.

(36) Huang, T. M.; You, Y. J.; Yang, C. S.; Tzeng, W. H.; Chen, J. T.; Cheng, M. C.; Wang, Y. *Organometallics* **1991**, *10*, 1020−1026.

(37) Merwin, R. K.; Roddick, D. M. *J. Organomet. Chem.* **1995**, *487*, 69−75.

(38) Mizuta, T.; Onishi, M.; Nakazono, T.; Nakazawa, H.; Miyoshi, K. *Organometallics* **2002**, *21*, 717−726.

(39) Michelin, R. A.; Mozzon, M.; Vialetto, B.; Bertani, R.; Bandoli, G.; Angelici, R. J. *Organometallics* **1998**, *17*, 1220−1226.

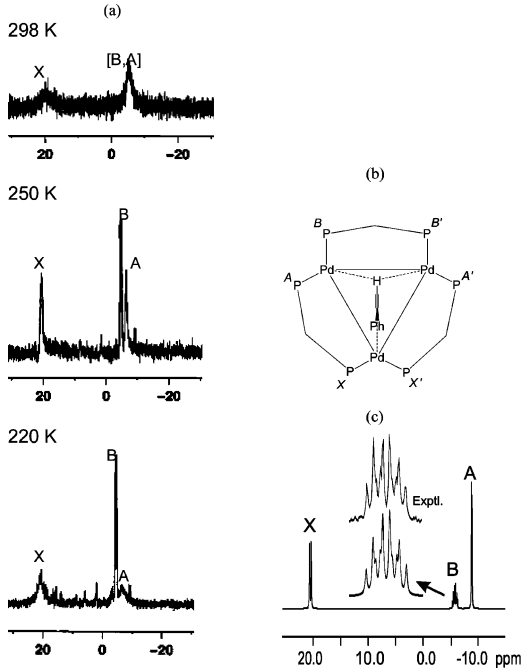

Figure 5. (a) Experimental ^{31}P NMR spectra presented as a function of temperature; (b) definition of the spin system (see text); (c) simulation of the 220 K spectrum in MestReC 4.9.9.6 with an expansion of the "B" resonance multiplet set beneath an expansion of the experimental "B" signal. The assignment of the peaks in the spectrum is tentative.

separation. Finally, we note that there is no evidence for a large (>400 Hz) coupling indicative of *trans* phosphines that result from a square-planar Pd environment. Taken as a whole, the complex ^{31}P NMR behavior may be, at first glance, indicative of a weaker interaction between Ph−C≡C−H and the Pd_3 cluster than for $MeO_2C-C\equiv C-CO_2Me$, but the high degree of fluxionality for Ph−C≡C−H renders the analysis more difficult.

A potential explanation for this is the following. The less activated Ph−C≡C−H competes less with CO for π-back-bonding, allowing CO to remain μ_3. This means that there is most likely no square-planar Pd (as seen in the NMR spectra for the $MeO_2C-C\equiv C-CO_2Me$ substrate). Presumably it is μ_2 to two Pd atoms, allowing it to be fluxional with C_s symmetry, as proposed, but just bound more strongly. This is so in the dication $[Pd_3(dppm)_3(CO)]^{2+}$; that is, the metal is electron poor and thus binds the more electron rich Ph−C≡C−H more strongly than the electron poorer $MeO_2C-C\equiv C-CO_2Me$. However, when $MeO_2C-C\equiv C-CO_2Me$ binds, it induces the shift in the CO group, leading to the lower symmetry complex with a square-planar Pd that we propose from ^{31}P NMR. This is at some energetic cost, reducing the overall equilibrium constant for this addition. Upon reduction, the metal becomes more electron rich, now the Ph−C≡C−H is even more strongly bound with greater π-back-bonding, and thus the EPR for $[Pd_3(dppm)_3(CO)]^{\bullet+}$ shows the low-symmetry spectrum.

Attempts to confirm this structural assignment by IR were inconclusive. The best spectra were obtained as KBr pellets; $[Pd_3(dppm)_3(CO)](PF_6)_2$ displayed a distinct ν(C≡O) band at 1840 cm^{-1} (cf. 1820 cm^{-1} reported for various salts of this dication[40]). The only evidence for a carbonyl stretch in $[Pd_3(dppm)_3(CO)(MeO_2C-C\equiv C-CO_2Me)](PF_6)_2$ is a shoulder to low energy (1700 cm^{-1}) of the ester carbonyl band at 1726 cm^{-1}; thus we cannot rule out an alternative structure in which the terminal ligand for the square-planar Pd is THF, and the CO ligand either is bridging the remaining two Pd atoms (cf. 1712 cm^{-1} in $[Pd_2(O_2CCF_3)_2(\mu\text{-CO})(\mu\text{-dppm})_2]$)[40] or is entirely dissociated, but retained in the proximity of the metal center by nonclassical interactions, e.g., with the ligand Ph groups. The fact remains that the addition and elimination of the alkynes in these systems is entirely reversible.

(40) Lloyd, B. R.; Puddephatt, R. J. *Inorg. Chim. Acta* **1984**, *90*, L77−L78.

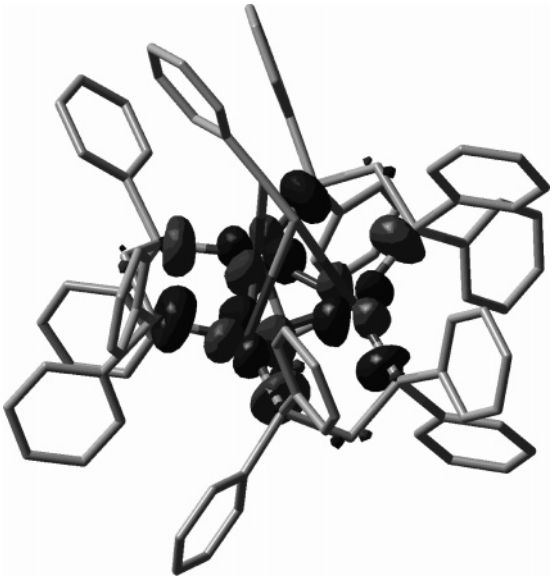

Figure 6. View of the SOMO for the optimized geometry of the Ph−C≡C−H/ $Pd_3(dppm)_3(CO)^+$ adduct (as one example; stick model). There is no chemical bonding between the Pd atoms and the C≡C moiety; the weak interactions are about 3.5 (Pd−C−Pd) and 4.0 (Pd−C) Å. These bonds were placed in the starting geometry assuming bonding distances.

DFT Calculations. DFT was used as a molecular modeling tool for the host−guest adduct *prior to activation.* For the Ph−C≡C−H case (as an example here and knowing that the species is fluxional), a nonclassical association (with the $[Pd_3(dppm)_3(CO)]^{\bullet+}$) is clearly computed where the substrate points inward toward the cavity by the small end (i.e., CH bond; Figure 6). The shortest Pd···C(substrate) distance is 3.5 Å, still a long value, clearly indicating weak interactions, presumably aided by hydrophobic phenyl−phenyl interactions. In addition, three P atoms are significantly displaced out of the original Pd_3P_6 plane, likely due to some steric hindrance to accommodate the guest molecule. To prove this, the Ph−C≡C−Ph substrate was also investigated by UV−vis and electrochemistry and did not exhibit any association at all. As a consequence for the Ph−C≡C−H case, the π-back-bonding interactions are decreased, hence easily explaining the shift of the reduction waves toward more negative potentials. The representation of the SOMO (also depicted in Figure 6) exhibits the same atomic contributions as for the "naked" monocation with *no spin density on the substrate*, reinforcing the weak nature of the host−guest interactions.

Characterization of the Paramagnetic Monocations. The bulk one-electron reductive electrolysis of $[Pd_3(dppm)_3(CO)(MeO_2C-C\equiv C-CO_2Me)]^{2+}$ and $[Pd_3(dppm)_3(CO)(Ph-C\equiv C-H)]^{2+}$ leads to the corresponding paramagnetic monocations, which are stable for several hours (the rate of decomposition could not be determined with accuracy) at 298 K in the absence

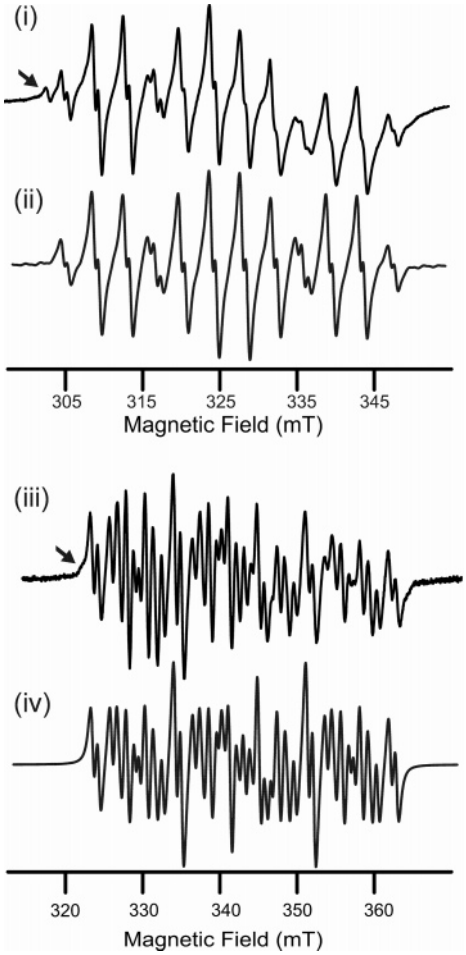

Figure 7. EPR spectra of (i) the $MeO_2C-C\equiv C-CO_2Me$/ and (iii) the $Ph-C\equiv C-H/Pd_3(dppm)_3(CO)^+$ adducts measured on extracts from the bulk electrolysis solutions in THF at room temperature. The experimental spectra have been corrected for a baseline drift, but are broadened at high field due to slow tumbling. The simulations (ii) and (iv) are performed in WinSim 0.98 (Public EPR Software Tools, NIEHS); see text for fitted parameters. The feature identified by the arrow in (i), which is not reflected in the high-field portion of the spectrum, is attributed to an impurity, but this signal obscures the weak satellite structure of the ^{105}Pd coupling; however, the feature identified in (iii) is in fact due to the contribution from this isotope (22.2% abundant).

of oxygen in THF (i.e., electrolytic solutions), in comparison with barely an hour for $[Pd_3(dppm)_3(CO)]^{\bullet+}$ (the EPR spectra were obtained *ex situ* by extracting aliquots from the bulk electrolysis experiments under careful protection from the atmosphere). Such stability is unprecedented. These same adducts are also obtained by first generating the $[Pd_3(dppm)_3(CO)]^{\bullet+}$ cluster by bulk electrolysis and then adding the organic substrates; identical EPR spectra are generated. The EPR spectra shown in Figure 7 are different from the symmetric septet of the $[Pd_3(dppm)_3(CO)]^+$ cluster (the EPR properties of which are $g = 2.065$, $A(^{31}P) = 75.8 \times 10^{-4}$ cm^{-1}, $A(^{105}Pd) = 7.6 \times 10^{-4}$ cm^{-1}).[4] The spectra cover a large field range (ca. 40 mT) and are appreciably line-broadened at high field. This is attributed to tumbling insufficiently fast to average out the anisotropy of the hyperfine coupling tensor, an effect commonly seen for large radicals covering large field/frequency ranges. Numerical fitting of the experimental spectrum of $[Pd_3(dppm)_3(CO)(MeO_2C-C\equiv C-CO_2Me)]^{\bullet+}$, after correction for baseline drift, using WinSim 0.98 software[41] converged with good agreement to $A(^{31}P) = 180.5$; 105.6; 3×37.9; 7.0×10^{-4} cm^{-1} with a line width of 5.5×10^{-4} cm^{-1}. The simulation also includes three $A(^{105}Pd) = 5.5 \times 10^{-4}$ cm^{-1}, but we cannot place any great confidence on the Pd hyperfine coupling constants and merely suggest that these new values are reasonable compared to those of the parent radical cation ($3 \times 7.6 \times 10^{-4}$ cm^{-1}). The isotropic g value is 2.038.

Despite its apparent complexity, the spectrum of $[Pd_3(dppm)_3(CO)(Ph-C\equiv C-H)]^{\bullet+}$ can be readily simulated as a cascading set of doublets due to the dominant ^{31}P contributions to the isotropic hyperfine coupling. Numerical fitting of the experimental spectrum, after correction for baseline drift, again using WinSim, converged with good agreement to $A(^{31}P) = 160.0$; 100.19; 43.0; 34.2, 23.0; 8.4×10^{-4} cm^{-1} with a line width of 4.8×10^{-4} cm^{-1}. The simulations give good agreement employing purely Lorentzian line shapes, indicative of the absence of further unresolved coupling, such as to the CH_2 hydrogens of the dppm ligands or the alkyne terminal hydrogen atom. The isotropic g value of 2.032 is quite similar to that of the other adduct, and both are considerably smaller than the 2.065 value recorded for the parent radical cation. A Pascal triangle illustrating the electron$-^{31}P$ hyperfine coupling is provided in the Supporting Information to reinforce this interpretation of the origin of the spectrum.

The low symmetry of the adducts on the EPR time scale is very consistent with the highly distorted crystal structure reported for the only structurally characterized complex of this kind, $[Pd_3(dppm)_3(O_2CCF_3)(MeO_2C-C\equiv C-CO_2Me)]^+$.[33] Apparently, the different magnetic environments experienced by the six P atoms result in significantly different spin densities or, alternatively, result in subtle differences in hybridization that affect the phosphorus s-components of the singly occupied molecular orbital in these complexes. Despite the very different appearances of the spectra of these two adducts, their $A(^{31}P)$ values are actually remarkably similar; each has one very large and one intermediate value, followed by three in the $(20-40) \times 10^{-4}$ cm^{-1} range, which happen to be identical for the $MeO_2C-C\equiv C-CO_2Me$ but give three different values in the $Ph-C\equiv C-H$ adduct. Moreover, there is one very small value. Finally, we note that despite the very dramatic shifts of the $A(^{31}P)$ from the six equivalent 75.8×10^{-4} cm^{-1} values in the parent radical cation, the sum of the $A(^{31}P)$ values are rather constant, coming to 369, 407, and 454×10^{-4} cm^{-1} for the $Ph-C\equiv C-H$ and $MeO_2C-C\equiv C-CO_2Me$ adducts and the parent radical cation, respectively. It is the partitioning of the unpaired spin density among the phosphorus and palladium atoms that varies from host to adduct to adduct. Note also that the smallish values of the $A(^{105}Pd)$ constants reflect the almost exactly 10-fold smaller nuclear gyromagnetic ratio of the latter compared to ^{31}P.

Conclusion

Our adducts in THF solutions exhibit complete reversibility in ethynyl−palladium interactions (i.e., substrate activation) for both states of charge (+2 and +1) and substantial enhanced stability of the corresponding paramagnetic $[Pd_3(dppm)_3(CO)]^+$ clusters going from less than an hour to several hours in the absence of oxygen. This gain in stability is interpreted to derive from screening of the very reactive Pd_3^+ center from the "outside

(41) O'Brian, D. A. D.; D. R.; Fann, Y. C. *Public EPR Software Tools*; National Institute of Environmental Health Sciences, National Institutes of Health.

world", here the solvent (and the supporting electrolyte when it applies). Solvent involvement, notably THF, in the reactivity of hydroxide anion with the "unprotected" $[Pd_3(dppm)_3(CO)]^+$ was recently demonstrated.[10] In addition to this evidence, both alkyne−$Pd_3(dppm)_3(CO)^{2+}$ adducts are found to be stable toward BPh_4^-; ordinarily $[Pd_3(dppm)_3(CO)]^{2+}$ is reduced to $[Pd_3(dppm)_3(CO)]^+$ in the presence of BPh_4^-.[7]

When we used methanol as the solvent, the electrochemical waves for the oxidation of the cluster−ethynyl adducts in cyclic voltammetry were irreversible, in strong contrast to the reversible behavior obtained using THF. This result corroborates Puddephatt's findings, but the reason for why this is so is still unknown to us. This work also introduces the concept of a molecular shuttle where a neutral substrate can be selectively bonded inside the cavity when the charge is +1, but is not favored when the charge is +2 in the presence of a stronger anionic guest (for example NO_3^-). Results from experiments exploiting this concept as well as the formation of adducts with a more diverse group of alkynes will be reported soon.

Experimental Section

Materials. The $[Pd_3(dppm)_3(CO)](PF_6)_2$ salt was prepared according to a literature procedure.[40,42] THF was distilled under Ar over Na-benzophenone. The alkyne substrates were purchased from Aldrich and were used as received.

Electrochemical Experiments. All manipulations were performed using Schlenk techniques in an atmosphere of dry oxygen-free argon. The supporting electrolyte was degassed under vacuum before use and then dissolved to a concentration of 0.2 mol·L^{-1}. For cyclic voltammetry experiments, the concentration of the analyte was almost 10^{-3} mol·L^{-1}. Voltammetric analyses were carried out in a standard three-electrode cell using an EG&G Princeton Applied Research (PAR) model 263A potentiostat, interfaced to a computer running Electrochemistry Power Suite software. The reference electrode was a saturated calomel electrode (SCE) separated from the solution by a sintered glass disk. The auxiliary electrode was a platinum wire. For all voltammetric measurements, the working electrode was a vitreous carbon disk (ϕ = 3 mm). Under these conditions, when operating in THF, the formal potential for the ferrocene (+/0) couple was found to be +0.56 V vs the SCE. The controlled potential electrolysis was performed with an Amel 552 potentiostat coupled with an Amel 721 electronic integrator. Bulk electrolyses were performed in a cell with three compartments separated with glass frits of medium porosity. Carbon gauze was used as the working electrode, a platinum plate as the counter electrode, and a saturated calomel electrode as the reference electrode.

Apparatus. The UV−vis spectra were acquired on a Varian CARY 50 spectrophotometer. Mass spectra were obtained on a Bruker ProFLEX III spectrometer (MALDI-TOF) using dithranol as matrix. The IR spectra were recorded on a Bruker Vector 22 FT-IR spectrophotmeter. The EPR spectra were acquired on a Bruker Elexsys E500 spectrometer. The NMR spectra were recorded on a 600 MHz Bruker Avance II NMR spectrometer. The chemical shifts are reported with respect to TMS (^{1}H NMR) and H_3PO_4 (^{31}P NMR).

Computational Details. The calculations were performed with Gaussian 03 revision C.02[43] at the B3LYP[44,45]level. Different basis sets were used depending on the type of atoms with the GEN[43] and PSEUDO=READ[43] keywords in order to address the large number of electrons per molecule. C, H, O were fully described with 6-31G[46] basis sets, and P was described with 3-21G*[47] basis sets and core pseudopotential, and the Pd's were described with LanL2dZ[48] basis sets and core pseudopotentials.

Acknowledgment. We are grateful to Drs. Jean-Claude Chambron and Michel Picquet (ICMUB, Dijon) for MALDI-TOF and NMR experiments, respectively. The Natural Sciences and Engineering Research Council of Canada (NSERC) and the Centre National de Recherche Scientifique (CNRS, UMR 5260) are acknowledged for funding.

Supporting Information Available: Pascal triangle explaining the electron−^{31}P coupling pattern for the paramagnetic $[Pd_3(dppm)_3(CO)]^+$/Ph−C≡C−H adduct.

OM700377A

(42) Manojlovic-Muir, L.; Muir, K. W.; Lloyd, B. R.; Puddephatt, R. J. *J. Chem. Soc., Chem. Commun.* **1983** (22), 1336−1337.

(43) Frisch, M. J.; Trucks, G. W.; Schlegel, H. B.; Scuseria, G. E.; Robb, M. A.; Cheeseman, J. R.; Montgomery, J. A., Jr.; Vreven, T.; Kudin, K. N.; Burant, J. C.; Millam, J. M.; Iyengar, S. S.; Tomasi, J.; Barone, V.; Mennucci, B.; Cossi, M.; Scalmani, G.; Rega, N.; Petersson, G. A.; Nakatsuji, H.; Hada, M.; Ehara, M.; Toyota, K.; Fukuda, R.; Hasegawa, J.; Ishida, M.; Nakajima, T.; Honda, Y.; Kitao, O.; Nakai, H.; Klene, M.; Li, X.; Knox, J. E.; Hratchian, H. P.; Cross, J. B.; Adamo, C.; Jaramillo, J.; Gomperts, R.; Stratmann, R. E.; Yazyev, O.; Austin, A. J.; Cammi, R.; Pomelli, C.; Ochterski, J. W.; Ayala, P. Y.; Morokuma, K.; Voth, G. A.; Salvador, P.; Dannenberg, J. J.; Zakrzewski, V. G.; Dapprich, S.; Daniels, A. D.; Strain, M. C.; Farkas, O.; Malick, D. K.; Rabuck, A. D.; Raghavachari, K.; Foresman, J. B.; Ortiz, J. V.; Cui, Q.; Baboul, A. G.; Clifford, S.; Cioslowski, J.; Stefanov, B. B.; Liu, G.; Liashenko, A.; Piskorz, P.; Komaromi, I.; Martin, R. L.; Fox, D. J.; Keith, T.; Al-Laham, M. A.; Peng, C. Y.; Nanayakkara, A.; Challacombe, M.; Gill, P. M. W.; Johnson, B.; Chen, W.; Wong, M. W.; Gonzalez, C.; Pople, J. A. *Gaussian*; Gaussian, Inc.: Wallingford, CT, 2004.

(44) Lee, C.; Yang, W.; Parr, R. G. *Phys. Rev. B: Condens. Matter Mater. Phys.* **1988**, *37*, 785−789.

(45) Miehlich, B.; Savin, A.; Stoll, H.; Preuss, H. *Chem. Phys. Lett.* **1989**, *157*, 200−206.

(46) Binkley, J. S.; Pople, J. A.; Hehre, W. J. *J. Am. Chem. Soc.* **1980**, *102*, 939−947.

(47) Ditchfield, R.; Hehre, W. J.; Pople, J. A. *J. Chem. Phys.* **1971**, *54*, 724−728.

(48) Hay, P. J.; Wadt, W. R. *J. Chem. Phys.* **1985**, *82*, 270−283.